# A database of marine and terrestrial radiogenic Nd and Sr isotopes for tracing earth-surface processes

Cécile L. Blanchet[1,2]

[1]Department of Geosciences, Freie Universität Berlin, Berlin, Germany
[2]Now at GFZ German Research Centre for Geosciences, Section 5.2 Climate Dynamics and Landscape Evolution, Potsdam, Germany

*Correspondence to*: Cécile L. Blanchet (blanchet@gfz-potsdam.de)

**Abstract.** The database presented here contains radiogenic neodymium and strontium isotope ratios measured on both terrestrial and marine sediments. The main purpose of this dataset is to help assessing sediment provenance and transport processes for various time intervals. This can be achieved by either mapping sediment isotopic signature and/or fingerprinting source areas using statistical tools.

The database has been built by incorporating data from the literature and the SedDB database and harmonizing the metadata, especially units and geographical coordinates. The original data were processed in three steps. Firstly, a specific attention has been devoted to provide geographical coordinates to each sample in order to be able to map the data. When available, the original geographical coordinates from the reference (generally DMS coordinates) were transferred into the decimal degrees system. When coordinates were not provided, an approximate location was derived from available information in the original publication. Secondly, all samples were assigned a set of standardized criteria that help splitting the dataset in specific categories. For instance, samples were discriminated according to their location "Region", "Sub-region" and "Location" that relate to location at continental to city/river scale) or the sample type (terrestrial samples - "aerosols", "soil sediments", "river sediments" - or marine samples - "marine sediment" or "trap sample"). Finally, samples were distinguished according to their deposition age, which allowed to compute average values for specific time intervals.

Graphical examples illustrating the functionality of the database are presented and the validity of the process was tested by comparing the results with published data. The dataset will be updated bi-annually and might be extended to reach a global geographical extent and/or add other type of samples. It is publicly available (under CC4.0-BY Licence) on the GFZ data management service at http://doi.org/10.5880/GFZ.5.2.2018.001.

# 1 Background and motivation

A large amount of sediments is deposited by rivers and winds on continental margins and in the deeper parts of marine basins. These deposits constitute very valuable climatic archives that are used in conjunction with terrestrial records and model outputs to better understand the climate-earth system. In that general context, the radiogenic isotopes of neodymium

(Nd) and strontium (Sr) measured in marine sediments have proven a powerful tool to determine their origin and their mode of transportation (i.e., fluvial or aeolian), related to climatic fluctuations (Frank, 2002). Neodymium isotope ratios are generally used to fingerprint provenance changes, as continental rocks have specific Nd isotopic signatures that are preserved during transportation and burial of sediments. Strontium isotope ratios are also sensitive provenance tracers, but

5    their original signature can be modified by weathering processes in the source area as well as grain-size sorting during sediment transportation. In conjunction with Nd isotopes, Sr isotope ratios therefore provide additional information on earth surface processes, such as changes in hydrological conditions, vegetation cover and modes of sediment transport.

The value of compiling Nd and Sr radioisotopes datasets has already been demonstrated by pioneering studies that investigated sediment generation and transport processes (Goldstein et al., 1984; Goldstein and O'Nions, 1981; Grousset et

10    al., 1988, 1990, 1992). More recently, several data compilations were used to trace submarine sediment transport processes in the Mediterranean (Krom et al., 1999b; Weldeab et al., 2002a) and fingerprint continental source areas (e.g., Padoan et al. (2011) for the Nile River basin and Scheuvens et al. (2013) for Northern Africa). The sedimentary database for geochemical analyses SedDB, which is hosted on the EarthChem platform, provides a large number of data for Nd and Sr isotopes (www.earthchem.org/seddb). This very useful instrument allows to sort data per type of analyses, age and location (among

15    other criteria) but has put on hold since 2013. It is therefore not up-to-date and does not integrate very important recent additions. Consequently, there is at present no combined dataset that allows to evaluate the contribution of specific sources to the sedimentary records and authors use parts of these datasets arbitrarily, based on their geographical relevance, together with their own discrete measurements (Blanchet et al., 2013; Castañeda et al., 2016; Revel et al., 2010; Wu et al., 2016). The lack of a comprehensive dataset therefore hinders the possibility of obtaining statistically significant estimations of source

20    contribution to the sediments and the use of harmonized identifiers for provenance.

I present here a compilation of published and unpublished data, which includes an integrated filtering system using criteria to subset the dataset. In addition to present-day measurements provided by the previously cited and additional studies, specific time-intervals were selected in order to plot and analyse paleo-data in the view of present-day values. This dataset is envisaged as an evolutive tool that will be bi-annually updated and will remain in the public domain. Other relevant proxies

25    and/or filtering criteria can be implemented in collaboration with peers.

In this paper, I will also present a few examples that illustrate the functionality of the database. Plotting has been realised with the freeware R and R scripts are also published to allow other users to subset and plot the data (Blanchet, 2018a, 2018b).


## 2. Methods

30    ### 2.1. Input data

The database has been built by incorporating data from the literature and the SedDB database and harmonizing the metadata, especially units and geographical coordinates. An overview of the input data is shown in Table 1. First, I used pre-existing

datasets from Padoan et al. (2011) and Scheuvens et al. (2013) (which included datasets from Krom et al. (1999b, 1999a) and Weldeab et al. (2002a, 2002b)). The focus of these studies is very different (resp., river runoff and dust characterization) but they are complementary and provide a large amount of data (resp., 86 and 192 data points). In a second time, 70 points were

5 retrieved from the SedDB database, which could be identified as core-tops and siliciclastic fraction (criteria set on Africa and Europe - 40ºS-55ºN; 35ºW-60ºN). Finally, a literature search has been conducted in order to add discrete samples that were not part of the previously-cited compilations (276 data points). Data were collected from 48 different references with a total of 631 data points (Table 1).

The database contains samples on which either the Nd or the Sr (or both) radiogenic isotope ratios were measured and expressed as εNd(0) and $^{87}Sr/^{86}Sr$. The notation εNd(0) is widely used and is calculated as:

10 $\varepsilon Nd(0) = [((^{143}Nd/^{144}Nd)_{sample}/(^{143}Nd/^{144}Nd)_{CHUR} - 1] * 10,000,$

where CHUR stands for chondritic uniform reservoir and has a $^{143}Nd/^{144}Nd$ ratio of 0.512638. When possible, I incorporated additional variables, such as the raw $^{143}Nd/^{144}Nd$ isotope ratio and the concentration in Sr and/or Nd in parts per million (ppm). As shown by Cole et al. (2009), sedimentary Nd and Sr concentrations can provide valuable clues for paleo-environmental interpretations.

15 **2.2. Data processing**

The original data were then processed in three steps, as shown in Table 1. Firstly, a specific attention has been devoted to provide geographical coordinates to each sample in order to be able to map the data (cf. Figure 1). When available, the original geographical coordinates from the reference (generally DMS coordinates, with different precision standard) were transferred into the decimal degrees system. When coordinates were not provided, I estimated an approximate location for

20 the samples from available information in the original publication. I generally used the maps or location information (e.g., cities), and determined the geographical location using online coordinate finders (e.g., https://www.latlong.net/).

In a second time, all samples were assigned a set of standardized criteria that help splitting the dataset in specific categories (Table 1). Samples were attributed criteria related to their location. The "Region" category provides a general sorting at continental or oceanic scale (e.g., "Mediterranean", "Atlantic", "Africa", "Europe") and the "Sub-region" category allows to

25 select only specific areas at oceanic sub-basins or country level (e.g., Mediterranean sub-basins or African countries). A third category "Location" permits to select specific areas or entities such as river basins or potential source areas (PSA) for dust production as defined in Scheuvens et al. (2013) (Figure 1). Criteria were also defined in order to select specific types of samples: terrestrial samples ("aerosols", "soil sediments", "river sediments", "bivalves") or marine samples ("marine sediment" or "trap sample") (Figure 1). I reported, when available, the grain-size fraction on which the measurements were

30 realised (bulk or fraction in μm), which can be useful to trace specific transportation modes (Blanchet et al., 2013).

Third, samples were discriminated according to their age and average values were computed for specific time intervals (Table 2). Most terrestrial samples are categorized as present-day samples but marine samples were sorted according to their age:

- Labelled as "P" (Present-day): I report here only surface seafloor samples for present-day sedimentation (i.e., generally core-top, the upper centimetre or past millennium). Sediment core samples that were collected bellow 1 cm or older as 1,000 years were not reported here as their value might be significantly different than present-day value, due to very different climatic and oceanographic conditions (e.g., see
5  values at 3-4 ka in Blanchet et al. (2014)).

- Labelled as "S1, S3, S4, S5, S6" (Sapropels): this refers to samples from the well-defined sapropel layers in the Mediterranean. Climatic and oceanic conditions are known to be radically different during these time intervals (with large freshwater delivery and low oxygen content in deeper parts of the Mediterranean Basin), which led to the occurrence of specific depositional environments (Rossignol-Strick, 1985). These
10  layers are generally visible (distinct black to grey-coloured sediments) in the sediment records and their extent is defined by specific geochemical tracers, such as the total organic carbon content or the barium concentration (De Lange et al., 2008). Using these markers and indications from the original publication, I calculated an average for these specific layers (used as a single value in the dataset). The depth or age interval used for the calculation, as well as number of sample and obtained average and standard deviation
15  ($2\sigma$) values are reported in table 2.

- Labelled as "LGM" (Last Glacial Maximum): samples of Last Glacial Maximum age (i.e., ca 20-25 ka BP) that were clearly identified in the original references were also added to the database. Related depth intervals and averaged values were determined in the cited publications (see Table 2).

## 3. Results

20  The dataset assembled includes the following fields for each sample:

- Name of the sample or sediment core,
- Criteria for location: Region, Sub-region, Location
- Sample type: soil sediment, river sediment, marine sediment, aerosol, trap sample,
- Grain-size fraction on which the measurements were done
25  - Criteria for time interval: present, sapropel layers, last glacial maximum,
- Concentration and isotopic ratio in Strontium and/or Neodymium in the detrital fraction
- Geographical coordinates: original longitude and latitude (from the reference publication) and longitude and latitude (in decimal degrees), as well as notes on coordinates,
- Notes on sample: specific information about the sample (from the reference publication),
30  - Reference: Original reference publication of the sample,
- Date of contribution: When the sample was added to the database,

– Source: Origin of the data point: Literature search, own (own measurements), sedDB (from the Sed Database, www.earthchem.org/seddb), Scheuvens et al. (2013), Padoan et al. (2011).


Table 3 provides an overview of the number of samples in the various categories defined in section 2.2. Most samples are located in Africa, the Atlantic Ocean and the Mediterranean Sea and represent the present-day sedimentation patterns. Most of the samples in the database are marine sediments and there is a significant contribution from river and soil sediments.

The sorting criteria allows users to select only a subset of the data and map the isotopic values (see Figures 2 and 3). As an example, I have reported in Table 3 the samples that originate from the different PSAs, which can then be used to evaluate their isotopic signature using standard statistical methods (see Figure 4).


## 4. Technical Validation

As the database is built by incrementing new measurements and homogenizing the metadata, one way to check its validity is to compare with previously published compilations.

Some of the earlier works that inspired and motivated this exercise are the mapping of Sr and Nd isotopes in seafloor sediments by Krom et al. (1999b) and Weldeab et al. (2002a). These studies were very innovative and provided a clear illustration of the role of continental sediment sources and land-to-sea transportation as well as submarine currents in building sedimentary deposits. It also highlighted the importance of accurately reconstructing present-day sedimentary dynamics to interpret the geological record. Both studies being (almost) twenty years old, the initial intention was to update their data compilation to integrate new measurements and generate more detailed maps of seafloor sediment signatures. The comparison between the original maps and new maps based on the database are presented in Figure 2. If the general pattern already identified by both studies (i.e., the large influence of Nile-derived sediment input on the eastern Levantine Basin) is reproduced by the new compilation, it allows to extend the record to the western part of the basin and unravel some new features. For instance, the updated maps demonstrate the influence of runoff from the Aegean sub-basin and the large impact of dust delivery on the Ionian sub-basin (with perhaps some local runoff from the Syrian and Tunisian coasts). Not shown here, the compilation and addition of sapropel layers also allows to map the effect of the increase in river runoff on the sedimentary signature of seafloor sediments.

Another motivation to build this database is the recent publication by Scheuvens et al. (2013), which provides a synoptic view on the geochemical signatures of potential source areas (PSA) for dust generation. In particular, this study compiled a large amount of data for Nd and Sr radioisotopes from soils, aerosols and marine sediments. I largely build on this compilation, which has been homogenized and completed with recent measurements, especially the Nile River sedimentary data from Padoan et al. (2011). One of the main modifications that was implemented is that I attributed approximate coordinates for samples with no given coordinate in the original reference. This was realised by using all available information, e.g., mention of cities or locations in the sample label or sample description, approximate location from the

published maps (see section 2.2). This operation was realized with great care as this is the main source of error and is clearly indicated in the database. It is however an important step as it allows to map contour lines that help unravelling features associated with earth surface processes (dust transportation, river runoff) that cannot be readily identified on maps in Scheuvens et al. (2013) (Figure 3).

5 The validity of the approach was controlled by comparing the values provided in Scheuvens et al. (2013) for the PSA to those that computed using the present dataset (Figure 4). Overall, the values obtained for each PSA are in good agreement with previous estimations. The integration of additional samples allowed to either confirm the observed values (e.g., for PSA1, PSA2 and PSA3) or to extend the value range and the number of data points (e.g., for PSA4, PSA5 and PSA6). One further advantage of using sorting criteria is that it allows to determine and plot statistics values associated with the PSAs

10 (Figure 4). The presented box plots allow to visualize the data range (as in Scheuvens et al., 2013) but also the skewness of the data (i.e., by looking at the difference between the mean in blue and the median, which is represented as the bar in the rectangles). The presence of outliers like in the Sr signature of PSA6 can be identified and dismissed from the source fingerprinting.

## 5. Data and code availability

15 The dataset of neodymium and strontium isotope ratios and associated metadata table as well as table 2 (determination of isotopic signature and identification of specific time intervals) and associated metadata table are available at http://doi.org/10.5880/GFZ.5.2.2018.001 (Blanchet, 2018c). The dataset and associated metadata are stored on GFZ Data Service as comma-separated files but it can also be provided as an excel file upon request.

All figures were realised using the R freeware (R Core Team, 2013). The R codes to reproduce maps in figures 1, 2 and 3 as

20 well as the box and whiskers plots in Figure 4 are available on Figshare (Blanchet, 2018a, 2018b).

## 6. Conclusion and outlook

The dataset assembled and presented here provides new insights into present and past earth-surface processes and the building of the marine sedimentary record. It allows to compare various types of sediments from the terrestrial to the marine realms: soils, deposited dust, river sediments, bivalves or marine sediments. The attribution of standardized geographical

25 locations enables to map the data and therefore to visualise sedimentary dynamics, while the use of sorting criteria related to the sample location or depositional age permits to determine source and sink isotopic signatures using statistical methods.

This database is thought as an evolving tool and is intended to grow as new measurements are published or provided by peers. Users are encouraged to contact the author (who will act as a curator) to submit new data and/or to propose any modification or improvement of the database. In that aim, an indication of entry date will be provided, which will help users

30 to follow the database updates and versions. It is intended that a bi-annual update will be provided.

**Competing interests**

The author declares that she has no conflict of interest.

**References**

Abouchami, W., Näthe, K., Kumar, A., Galer, S. J. G., Jochum, K. P., Williams, E., Horbe, A. M. C., Rosa, J. W. C., Balsam, W., Adams, D., Mezger, K. and Andreae, M. O.: Geochemical and isotopic characterization of the Bodélé
10   Depression dust source and implications for transatlantic dust transport to the Amazon Basin, Earth Planet. Sci. Lett., 380, 112–123, doi:10.1016/j.epsl.2013.08.028, 2013.

Blanchet, C.: R Code for mapping (contour maps) the Nd and Sr isotopic signature of marine and terrestrial sediments, Figshare, doi:10.6084/m9.figshare.6990161.v3, 2018a.

Blanchet, C.: R Code for plotting statistical parameters of Nd and Sr isotopic signature of Potential Source Areas, Figshare,
15   doi:10.6084/m9.figshare.6990260.v3, 2018b.

Blanchet, C. L.: A global database of radiogenic Nd and Sr isotopes in marine and terrestrial samples. V. 1. GFZ Data Service, 2018c. doi: 10.5880/GFZ.5.2.2018.001

Blanchet, C. L., Tjallingii, R., Frank, M., Lorenzen, J., Reitz, A., Brown, K., Feseker, T. and Brückmann, W.: High- and low-latitude forcing of the Nile River regime during the Holocene inferred from laminated sediments of the Nile deep-sea
20   fan, Earth Planet. Sci. Lett., 364, 98–110, doi:10.1016/j.epsl.2013.01.009, 2013.

Blanchet, C. L., Frank, M. and Schouten, S.: Asynchronous Changes in Vegetation, Runoff and Erosion in the Nile River Watershed during the Holocene, PLOS ONE, 9(12), e115958, doi:10.1371/journal.pone.0115958, 2014.

Box, M. R., Krom, M. D., Cliff, R. A., Bar-Matthews, M., Almogi-Labin, A., Ayalon, A. and Paterne, M.: Response of the Nile and its catchment to millennial-scale climatic change since the LGM from Sr isotopes and major elements of East
25   Mediterranean sediments, Quat. Sci. Rev., 30(3–4), 431–442, doi:10.1016/j.quascirev.2010.12.005, 2011.

Castañeda, I. S., Schouten, S., Pätzold, J., Lucassen, F., Kasemann, S., Kuhlmann, H. and Schefuß, E.: Hydroclimate variability in the Nile River Basin during the past 28,000 years, Earth Planet. Sci. Lett., 438, 47–56, doi:10.1016/j.epsl.2015.12.014, 2016.

Cole, J. M., Goldstein, S. L., deMenocal, P. B., Hemming, S. R. and Grousset, F. E.: Contrasting compositions of Saharan
30   dust in the eastern Atlantic Ocean during the last deglaciation and African Humid Period, Earth Planet. Sci. Lett., 278(3–4), 257–266, doi:10.1016/j.epsl.2008.12.011, 2009.

De Lange, G. J., Thomson, J., Reitz, A., Slomp, C. P., Speranza Principato, M., Erba, E. and Corselli, C.: Synchronous basin-wide formation and redox-controlled preservation of a Mediterranean sapropel, Nat. Geosci., 1(9), 606–610, doi:10.1038/ngeo283, 2008.

5   Frank, M.: Radiogenic isotopes: Tracers of past ocean circulation and erosional input, Rev. Geophys., 40(1), doi:10.1029/2000RG000094, 2002.

Franzese, A. M., Hemming, S. R., Goldstein, S. L. and Anderson, R. F.: Reduced Agulhas Leakage during the Last Glacial Maximum inferred from an integrated provenance and flux study, Earth Planet. Sci. Lett., 250(1), 72–88, doi:10.1016/j.epsl.2006.07.002, 2006.

Franzese, A. M., Hemming, S. R. and Goldstein, S. L.: Use of strontium isotopes in detrital sediments to constrain the glacial
10   position of the Agulhas Retroflection, Paleoceanography, 24(2), doi:10.1029/2008PA001706, 2009.

Freydier, R., Michard, A., De Lange, G. and Thomson, J.: Nd isotopic compositions of Eastern Mediterranean sediments: tracers of the Nile influence during sapropel S1 formation?, Mar. Geol., 177(1), 45–62, doi:doi:10.1016/S0025-3227(01)00123-2, 2001., 2001.

Goldstein, S. L. and O'Nions, R. K.: Nd and Sr isotopic relationships in pelagic clays and ferromanganese deposits, Nature,
15   292(5821), 324–327, doi:10.1038/292324a0, 1981.

Goldstein, S. L., O'Nions, R. K. and Hamilton, P. J.: A Sm-Nd isotopic study of atmospheric dusts and particulates from major river systems, Earth Planet. Sci. Lett., 70(2), 221–236, doi:10.1016/0012-821X(84)90007-4, 1984.

Gross, A., Palchan, D., Krom, M. D. and Angert, A.: Elemental and isotopic composition of surface soils from key Saharan dust sources, Chem. Geol., 442, 54–61, doi:10.1016/j.chemgeo.2016.09.001, 2016.

20   Grousset, F. E. and Biscaye, P. E.: Tracing dust sources and transport patterns using Sr, Nd and Pb isotopes, Chem. Geol., 222(3–4), 149–167, doi:10.1016/j.chemgeo.2005.05.006, 2005.

Grousset, F. E., Biscaye, P. E., Zindler, A., Prospero, J. and Chester, R.: Neodymium isotopes as tracers in marine sediments and aerosols: North Atlantic, Earth Planet. Sci. Lett., 87(4), 367–378, doi:https://doi.org/10.1016/0012-821X(88)90001-5, 1988.

25   Grousset, F. E., Henry, F., Minster, J. F. and Monaco, A.: Nd isotopes as tracers in water column particles: the western Mediterranean Sea, Mar. Chem., 30, 389–407, doi:10.1016/0304-4203(90)90083-O, 1990.

Grousset, F. E., Rognon, P., Coudé-Gaussen, G. and Pédemay, P.: Origins of peri-Saharan dust deposits traced by their Nd and Sr isotopic composition, Palaeogeogr. Palaeoclimatol. Palaeoecol., 93(3), 203–212, doi:10.1016/0031-0182(92)90097-O, 1992.

30   Grousset, F. E., Parra, M., Bory, A., Martinez, P., Bertrand, P., Shimmield, G. and Ellam, R. M.: Saharan wind regimes traced by the Sr–Nd isotopic composition of subtropical Atlantic sediments: last glacial maximum vs today, Quat. Sci. Rev., 17(4), 395–409, doi:https://doi.org/10.1016/S0277-3791(97)00048-6, 1998.

Hemming, S. R., Flierdt, T. van de, Goldstein, S. L., Franzese, A. M., Roy, M., Gastineau, G. and Landrot, G.: Strontium isotope tracing of terrigenous sediment dispersal in the Antarctic Circumpolar Current: Implications for constraining frontal
35   positions, Geochem. Geophys. Geosystems, doi:https://doi.org/10.1029/2006GC001441, 2007.

Jung, S. J. A., Davies, G. R., Ganssen, G. M. and Kroon, D.: Stepwise Holocene aridification in NE Africa deduced from dust-borne radiogenic isotope records, Earth Planet. Sci. Lett., 221(1–4), 27–37, doi:10.1016/S0012-821X(04)00095-0, 2004.

5    Krom, M. D., Michard, A., Cliff, R. al and Strohle, K.: Sources of sediment to the Ionian Sea and western Levantine basin of the Eastern Mediterranean during S-1 sapropel times, Mar. Geol., 160(1), 45–61, doi:https://doi.org/10.1016/S0025-3227(99)00015-8, 1999a.

Krom, M. D., Cliff, R. A., Eijsink, L. M., Herut, B. and Chester, R.: The characterisation of Saharan dusts and Nile particulate matter in surface sediments from the Levantine basin using Sr isotopes, Mar. Geol., 155(3), 319–330, doi:https://doi.org/10.1016/S0025-3227(98)00130-3, 1999b.

10   Krom, M. D., Stanley, J. D., Cliff, R. A. and Woodward, J. C.: Nile River sediment fluctuations over the past 7000 yr and their key role in sapropel development, Geology, 30(1), 71, doi:https://doi.org/10.1130/0091-7613(2002)030<0071:NRSFOT>2.0.CO;2, 2002.

Osborne, A. H., Vance, D., Rohling, E. J., Barton, N., Rogerson, M. and Fello, N.: A humid corridor across the Sahara for the migration of early modern humans out of Africa 120,000 years ago, Proc. Natl. Acad. Sci., 105(43), 16444–16447, 15   doi:https://doi.org/10.1073/pnas.0804472105, 2008.

Padoan, M., Garzanti, E., Harlavan, Y. and Villa, I. M.: Tracing Nile sediment sources by Sr and Nd isotope signatures (Uganda, Ethiopia, Sudan), Geochim. Cosmochim. Acta, 75(12), 3627–3644, doi:10.1016/j.gca.2011.03.042, 2011.

Palchan, D., Stein, M., Almogi-Labin, A., Erel, Y. and Goldstein, S. L.: Dust transport and synoptic conditions over the Sahara–Arabia deserts during the MIS6/5 and 2/1 transitions from grain-size, chemical and isotopic properties of Red Sea 20   cores, Earth Planet. Sci. Lett., 382, 125–139, doi:https://doi.org/10.1016/j.epsl.2013.09.013, 2013.

R Core Team: R: A language and environment for statistical  computing, R Foundation for Statistical Computing, Vienna, Austria. [online] Available from: http://www.R-project.org/, 2013.

Revel, M., Ducassou, E., Grousset, F. E., Bernasconi, S. M., Migeon, S., Revillon, S., Mascle, J., Murat, A., Zaragosi, S. and Bosch, D.: 100,000 Years of African monsoon variability recorded in sediments of the Nile margin, Quat. Sci. Rev., 29(11–25   12), 1342–1362, doi:10.1016/j.quascirev.2010.02.006, 2010.

Revel, M., Colin, C., Bernasconi, S., Combourieu-Nebout, N., Ducassou, E., Grousset, F. E., Rolland, Y., Migeon, S., Bosch, D., Brunet, P., Zhao, Y. and Mascle, J.: 21,000 Years of Ethiopian African monsoon variability recorded in sediments of the western Nile deep-sea fan, Reg. Environ. Change, 14(5), 1685–1696, doi:10.1007/s10113-014-0588-x, 2014.

30   Revel, M., Ducassou, E., Skonieczny, C., Colin, C., Bastian, L., Bosch, D., Migeon, S. and Mascle, J.: 20,000 years of Nile River dynamics and environmental changes in the Nile catchment area as inferred from Nile upper continental slope sediments, Quat. Sci. Rev., 130, 200–221, doi:10.1016/j.quascirev.2015.10.030, 2015.

Révillon, S., Jouet, G., Bayon, G., Rabineau, M., Dennielou, B., H?mond, C. and Bern?, S.: The provenance of sediments in the Gulf of Lions, western Mediterranean Sea: SEDIMENTS IN THE GULF OF LIONS, Geochem. Geophys. Geosystems, 35   12(8), n/a-n/a, doi:10.1029/2011GC003523, 2011.

Rossignol-Strick, M.: Mediterranean Quaternary sapropels, an immediate response of the African monsoon to variation of insolation, Palaeogeogr. Palaeoclimatol. Palaeoecol., 49(3–4), 237–263, doi:10.1016/0031-0182(85)90056-2, 1985.

Scheuvens, D., Schütz, L., Kandler, K., Ebert, M. and Weinbruch, S.: Bulk composition of northern African dust and its source sediments — A compilation, Earth-Sci. Rev., 116, 170–194, doi:10.1016/j.earscirev.2012.08.005, 2013.

Stein, M., Almogi-Labin, A., Goldstein, S. L., Hemleben, C. and Starinsky, A.: Late Quaternary changes in desert dust inputs to the Red Sea and Gulf of Aden from 87Sr/86Sr ratios in deep-sea cores, Earth Planet. Sci. Lett., 261(1), 104–119, doi:10.1016/j.epsl.2007.06.008, 2007.

Weldeab, S., Emeis, K.-C., Hemleben, C. and Siebel, W.: Provenance of lithogenic surface sediments and pathways of riverine suspended matter in the Eastern Mediterranean Sea: evidence from 143 Nd/144 Nd and 87 Sr/86 Sr ratios, Chem. Geol., 186(1), 139–149, doi:https://doi.org/10.1016/S0009-2541(01)00415-6, 2002a.

Weldeab, S., Emeis, K.-C., Hemleben, C., Vennemann, T. W. and Schulz, H.: Sr and Nd isotope composition of Late Pleistocene sapropels and nonsapropelic sediments from the Eastern Mediterranean Sea: implications for detrital influx and climatic conditions in the source areas, Geochim. Cosmochim. Acta, 66(20), 3585–3598, doi:https://doi.org/10.1016/S0016-7037(02)00954-7, 2002b.

Wu, J., Böning, P., Pahnke, K., Tachikawa, K. and de Lange, G. J.: Unraveling North-African riverine and eolian contributions to central Mediterranean sediments during Holocene sapropel S1 formation, Quat. Sci. Rev., 152, 31–48, doi:10.1016/j.quascirev.2016.09.029, 2016.

**Tables**

| Source | Characteristics | Data characteristics | Attribution / harmonization of coordinates | Attribution of sorting criteria | Determination of specific time interval | Number of data points |
|---|---|---|---|---|---|---|
| Padoan | Research article | River sed. | YES | YES | NO | 86 |
| Scheuvens | Review article | Aerosols, marine sed., river sed., soils, trap sample | YES | YES | YES | 192 |
| SedDB* | Database | Sedimentary database | YES | YES | YES | 70 |
| Literature search** | Peer-reviewed publications | Sediment Nd and Sr isotopic signatures | YES | YES | YES | 276 |
| Own data*** | Own research articles and own measurements | Sediment Nd and Sr isotopic signatures | NO | YES | YES | 7 |
| Total | | | | | | 631 |

**Table 1: Data input sources and type of data provided. First column shows the input sources (Padoan et al., 2011 and Scheuvens et al., 2013), *SedDB at www.earthchem.org/seddb, **Reference list for the dataset available at Data Citation 1, *** Own data from ref. 18 and Blanchet et al. in prep.). Indications about the type of source, the characteristics of the data retrieved are provided. The data was then submitted to three processes: sorting criteria were attributed to all the samples, a homogenous geographical location (coordinates in decimal degrees) was attributed or to some samples and the isotopic values of specific time intervals was determined when possible (see "Methods" section for further information).**

| Label | Time interval | Core depth interval (cm) | Duration (kyr) | n | $^{87}Sr/^{86}Sr$ | $2\sigma$ | $\epsilon Nd(0)$ | $2\sigma$ | Identifier | Ref. |
|---|---|---|---|---|---|---|---|---|---|---|

| | | | | | | | | | | |
|---|---|---|---|---|---|---|---|---|---|---|
| P362/2-33 | S1 | 50-551 | 6.11-9.53 | 22 | 0.70876 | 0.00126 | -3.80 | 0.71 | visual, geochemical (TOC, Ba/Al) | 1 |
| 64PE349-8 | S1 | 20-30 | 5.04-8.32 | 3 | 0.71608 | 0.00101 | -10.65 | 0.98 | visual, geochemical (TOC, Ba/Al) | 2 |
| 9501 | S1 | 64-87 | 6.49-9.93 | 12 | 0.71072 | 0.00036 | | | geochemical (TOC, Ba/Al) | 3 |
| 9509 | S1 | 100-180 | 6.17-9.97 | 13 | 0.70952 | 0.00032 | | | geochemical (TOC, Ba/Al) | 3 |
| GeoB7702-3 | S1 | 2.46-2.58 | 8.66-9.88 | 2 | 0.70900 | 0.00000 | -4.64 | 0.33 | geochemical (biomarkers) | 4 |
| ODP Leg 108, Site 658C | S1 | 1.35-2.02 | 6.06-9.82 | 19 | 0.71653 | 0.00125 | -14.33 | 0.23 | Age - African Humid Period | 5 |
| UM42 | S1 | 22.15-27.65 | | 6 | 0.71581 | 0.00060 | -11.48 | 0.52 | Geochemical (Ba/Al) | |
| BC3 | S1 | 12.8-21.2 | | 5 | 0.71604 | 0.00075 | -10.82 | 0.26 | Geochemical (Ba/Al) | |
| BC19 | S1 | 23.25-30.25 | | 5 | 0.71179 | 0.00054 | -8.16 | 0.30 | Geochemical (Ba/Al) | 6 |
| BC07 | S1 | 15.25-36.25 | | 8 | 0.71122 | 0.00017 | -8.46 | 0.36 | Geochemical (Ba/Al) | |
| SL114 | S1 | 24.05-34.05 | | 4 | 0.71607 | 0.00058 | -10.35 | 0.31 | Geochemical (Ba/Al) | |
| Core NIOP 905 P | S1 | | 6.43-9.53 | 81 | 0.71426 | 0.00032 | -5.91 | 0.25 | Age - African Humid Period | 7 |
| UM35 | S1 | 19.25-26.25 | | 5 | 0.71524 | 0.00125 | | | Geochemical (TOC) | |
| Stn 20 | S1 | 19.5-24.5 | | 3 | 0.71408 | 0.00305 | | | Geochemical (TOC) | |
| ABC26 | S1 | 22.6-25.8 | | 3 | 0.71483 | 0.00266 | | | Geochemical (TOC) | 8 |
| MC12 | S1 | 23.1-27.1 | | 2 | 0.71317 | 0.00074 | | | Geochemical (TOC) | |
| KC01 | S1 | 11.8-13.0 | | 4 | 0.71372 | 0.00126 | | | Geochemical (TOC) | |
| BC19 | S1 | 27-35 | | 3 | 0.70978 | 0.00013 | | | Geochemical (TOC) | |
| Cores s-21 | S1 | Determined in publication | >6 | 4 | 0.70880 | | | | Age - African Humid Period | 9 |
| MS27PT | S1 | 23-294 | 6.15-14.26 | 55 | 0.70860 | 0.00105 | -4.99 | 1.10 | visual, geochemical (TOC, Ba/Al) | 10, 11 |
| MD04-2622 | S1 | 113-121 | 9.9-10.0 | 2 | 0.70909 | 0.00008 | -6.16 | 0.03 | visual, geochemical (TOC, Ba/Al) | 11 |
| MD04-2627 | S1 | 75-111 | 6.01-10.27 | 20 | | | -3.81 | 0.67 | visual, geochemical (TOC, Ba/Al) | 11 |
| KSGC31-671 | S1 | 671 | 8.94 | 1 | 0.71716 | | -10.9 | | Age - African Humid Period | 12 |
| KL11 | S1 | 64-65 | 6 | 1 | 0.70831 | | | | Age - African Humid Period | 13 |
| KL15 | S1 | 41-42 | 6.6 | 1 | 0.70968 | | | | Age - African Humid Period | 13 |
| CP10BC | S1 | 21.25-34.75 | 6.2-9.6 | 16 | 0.71604 | 0.00104 | -11.17 | 0.30 | visual, geochemical (TOC, Ba/Al) | 14 |
| RC14-11 | LGM | Determined in publication | | | 0.71020 | | | | Age - LGM | 15 |

| | | | | | | | | | | |
|---|---|---|---|---|---|---|---|---|---|---|
| VM24-203 | LGM | Determined in publication | | | 0.70620 | | | | Age - LGM | |
| RC13-243 | LGM | Determined in publication | | | 0.71305 | | -6.43 | | Age - LGM | |
| RC11-86 | LGM | Determined in publication | | | 0.72696 | | -10.17 | | Age - LGM | |
| VM24-231 | LGM | Determined in publication | | | 0.70980 | | | | Age - LGM | |
| RC17-69 | LGM | Determined in publication | | | 0.72391 | | -11.72 | | Age - LGM | |
| VM19-240 | LGM | Determined in publication | | | 0.72307 | | -9.65 | | Age - LGM | |
| VM14-77 | LGM | Determined in publication | | | 0.72861 | | -16.08 | | Age - LGM | |
| RC13-229 | LGM | Determined in publication | | | 0.71852 | | -9.43 | | Age - LGM | |
| RC8-19 | LGM | Determined in publication | | | 0.71190 | | | | Age - LGM | |
| VM19-214 | LGM | Determined in publication | | | 0.73369 | | -14.78 | | Age - LGM | |
| RC13-227 | LGM | Determined in publication | | | 0.72108 | | -10.12 | | Age - LGM | |
| VM34-153 | LGM | Determined in publication | | | 0.71830 | | | | Age - LGM | |
| RC11-87 | LGM | Determined in publication | | | 0.71614 | | | | Age - LGM | |
| VM16-53 | LGM | Determined in publication | | | 0.71853 | | | | Age - LGM | |
| VM20-201 | LGM | Determined in publication | | | 0.71923 | | | | Age - LGM | |
| VM19-224 | LGM | Determined in publication | | | 0.71696 | | | | Age - LGM | |
| RC14-3 | LGM | Determined in publication | | | 0.71668 | | | | Age - LGM | |
| CD154-13-12K | LGM | Determined in publication | | | 0.72054 | | | | Age - LGM | |
| CD154-15-14K | LGM | Determined in publication | | | 0.71592 | | | | Age - LGM | |
| CD154-15-13K | LGM | Determined in publication | | | 0.71632 | | | | Age - LGM | 16 |
| CD154-16-15K | LGM | Determined in publication | | | 0.71820 | | | | Age - LGM | |
| CD154-15-12PK | LGM | Determined in publication | | | 0.71893 | | | | Age - LGM | |
| CD154-09-9PK | LGM | Determined in publication | | | 0.72258 | | | | Age - LGM | |
| CD154-06-6PK | LGM | Determined in publication | | | 0.72476 | | | | Age - LGM | |
| CD154-02-3K | LGM | Determined in publication | | | 0.73075 | | | | Age - LGM | |
| VM30-41K | LGM | Determined in publication | | | 0.71747 | | -11.40 | | Age - LGM | 17 |
| VM22-189 | LGM | Determined in publication | | | 0.71805 | | -13.80 | | Age - LGM | |

| VM27-175 | LGM | Determined in publication | | | 0.71848 | | -15.90 | | Age - LGM | |
|---|---|---|---|---|---|---|---|---|---|---|
| VM22-196 | LGM | Determined in publication | | | 0.71991 | | -18.30 | | Age - LGM | |
| 31 | LGM | Determined in publication | | | 0.71744 | | -13.30 | | Age - LGM | |
| K02 | LGM | Determined in publication | | | 0.72308 | | -17.80 | | Age - LGM | |
| 29 | LGM | Determined in publication | | | 0.71744 | | -13.70 | | Age - LGM | |
| K11 | LGM | Determined in publication | | | 0.71699 | | -17.90 | | Age - LGM | |
| 32 | LGM | Determined in publication | | | 0.72093 | | -13.10 | | Age - LGM | |
| K15 | LGM | Determined in publication | | | 0.71904 | | -19.50 | | Age - LGM | |
| 28 | LGM | Determined in publication | | | 0.72044 | | -12.40 | | Age - LGM | |
| K20b | LGM | Determined in publication | | | 0.71933 | | -14.10 | | Age - LGM | |
| K17d | LGM | Determined in publication | | | 0.71632 | | | | Age - LGM | |
| RC14-11 | LGM | Determined in publication | | | 0.71024 | | | | Age - LGM | 18 |
| V24-203 | LGM | Determined in publication | | | 0.70622 | | | | Age - LGM | 18 |
| KL23 | LGM | Determined in publication | | | 0.71113 | | -5.68 | | Age - LGM | 19 |
| 64PE349-8 | S3 | 240 | 83.94 | 2 | 0.71427 | 0.00066 | -11.31 | 0.21 | visual, geochemical (TOC, Ba/Al) | 2 |
| 64PE349-8 | S4 | 280-300 | 102.46-110.66 | 4 | 0.71499 | 0.00168 | -9.85 | 1.70 | visual, geochemical (TOC, Ba/Al) | |
| 64PE349-8 | S5 | 345-375 | 126.81-138.83 | 6 | 0.71518 | 0.00112 | -11.02 | 0.66 | visual, geochemical (TOC, Ba/Al) | |
| SL71 | S5 | 263.-275.5 | | 4 | 0.71129 | 0.00074 | -8.00 | 0.50 | visual, geochemical (d18O) | 20 |
| SL67 | S5 | 386.5-446.5 | | 4 | 0.71039 | 0.00024 | -7.45 | 0.06 | visual, geochemical (d18O) | |
| KL83 | S5 | 398-414 | | 4 | 0.70931 | 0.00003 | -5.13 | 0.19 | visual, geochemical (d18O) | |
| SL71 | S6 | 387.5-4145 | | 4 | 0.71231 | 0.00075 | -8.58 | 0.75 | visual, geochemical (d18O) | |
| KL51 | S6 | 535.5-573.5 | | 4 | 0.71164 | 0.00042 | -7.98 | 0.28 | visual, geochemical (d18O) | |
| KL83 | S6 | 566-618 | | 6 | 0.70907 | 0.00019 | -4.20 | 0.25 | visual, geochemical (d18O) | |

**Table 2: Identification of specific time intervals (sapropel layers and last glacial maximum) in marine sediments. Headers from left to right: Label = name of the sediment core; Time interval = sapropel layers S1, S3, S4, S5 and S6 and last glacial maximum LGM; Core depth interval (cm) and corresponding Duration (kyr); n = Number of samples; Averages and Standard deviations (2σ) for Sr and Nd isotope ratios (with Nd isotopes expressed as εNd(0)); Identifier = measurement or method used to determine the extent of the specific time interval; Ref. = Reference publications. 1: Blanchet et al. (2014), 2: Blanchet et al. (in prep.), 3: Box et al. (2011), 4: Castañeda et al. (2016), 5: Cole et al. (2009), 6: Freydier et al. (2001), 7: Jung et al. (2004), 8: Krom et al. (1999a), 9: Krom et al. (2002), 10: Revel et al. (2010, 2014), 11: Revel et al. (2015), 12: Révillon et al. (2011), 13: Stein et al. (2007), 14: Wu et**

al. (2016), 15: Franzese et al. (2006), 16: Franzese et al. (2009), 17: Grousset et al. (1998), 18: Hemming et al. (2007), 19: Palchan et al. (2013), 20: Weldeab et al. (2002b).

| Label | Sub-region | Location | Sample type | 87Sr/86Sr | eNd(0) | Longitude (Dec. degrees) | Latitude (Dec. degrees) | Ref. |
|---|---|---|---|---|---|---|---|---|
| TUI78 | Tunisia | PSA1 | soil sediment | 0.71424 | -9.5 | 9.78 | 34.20 | 1 |
| Algeria | Algeria | PSA1 | soil sediment | | -13.5 | 3.14 | 35.57 | 2 |
| Senegal River | Senegal | PSA2 | river sediment | 0.72858 | -13.1 | -15.00 | 16.60 | |
| Kiffa | Mauritania | PSA2 | soil sediment | 0.72839 | -13.9 | -11.40 | 16.60 | |
| Nouakchott | Mauritania | PSA2 | soil sediment | 0.72002 | -15.9 | -15.95 | 18.07 | |
| Erg Sud Atar | Mauritania | PSA2 | soil sediment | 0.73765 | -13.5 | -12.70 | 21.30 | 3 |
| Atar | Mauritania | PSA2 | soil sediment | 0.72728 | -17.9 | -11.80 | 21.90 | |
| Zouerat | Mauritania | PSA2 | soil sediment | 0.73568 | -17.8 | -10.90 | 23.80 | |
| Essmarra | Morocco | PSA2 | soil sediment | 0.73404 | -16.3 | -10.36 | 27.78 | |
| JB | Moroco | PSA2 | soil sediment | 0.72194 | -14.0 | -5.62 | 29.93 | |
| IR | Morocco | PSA2 | soil sediment | 0.72565 | -13.8 | -6.58 | 29.98 | 4 |
| EM | Morocco | PSA2 | soil sediment | 0.72764 | -13.0 | -5.62 | 30.35 | |
| ATK-35 (Atakor) | Algeria | PSA3 | soil sediment | | -12.1 | 1.21 | 28.19 | |
| MEK-21 (Sebkra Mekkerane) | Algeria | PSA3 | soil sediment | 0.72052 | | 1.66 | 28.03 | 3 |
| MEK-58 (Sebkra Mekkerane) | Algeria | PSA3 | soil sediment | 0.72440 | | 1.66 | 28.03 | |
| Libya2 | Libya | PSA4 | soil sediment | | -13.8 | 16.98 | 28.03 | 2 |
| Libya4 | Libya | PSA4 | soil sediment | 0.71521 | -10.7 | 18.26 | 26.59 | 2 |
| N26 | Libya | PSA4 | soil sediment | 0.70651 | -3.8 | 16.57 | 25.58 | 5 |
| Chad | Chad | PSA5 | soil sediment | | -12.7 | 13.95 | 14.35 | 2 |
| Bod 43.5 | Chad | PSA5 | soil sediment | | -13.1 | 18.55 | 16.10 | |
| Bod 43.5_duplicate | Chad | PSA5 | soil sediment | 0.72833 | -12.7 | 18.55 | 16.10 | |
| Bod 44 | Chad | PSA5 | soil sediment | 0.71498 | -10.2 | 18.84 | 16.17 | |
| Bod 44B | Chad | PSA5 | soil sediment | 0.71477 | -10.1 | 18.84 | 16.17 | |
| Bod 54A | Chad | PSA5 | soil sediment | 0.72908 | -13.1 | 18.61 | 16.20 | |
| Bod 54A_duplicate | Chad | PSA5 | soil sediment | 0.72931 | -12.7 | 18.61 | 16.20 | 6 |
| Bod 54B | Chad | PSA5 | soil sediment | | -12.8 | 18.61 | 16.20 | |
| Bod 54B_duplicate | Chad | PSA5 | soil sediment | 0.72761 | -12.9 | 18.61 | 16.20 | |
| Bod 44C | Chad | PSA5 | soil sediment | | -13.0 | 18.71 | 16.29 | |
| Bod 44D | Chad | PSA5 | soil sediment | 0.72794 | | 18.71 | 16.29 | |
| Bod 44D_duplicate | Chad | PSA5 | soil sediment | 0.72791 | -12.9 | 18.71 | 16.29 | |
| BODI | Chad | PSA5 | soil sediment | 0.71858 | -11.9 | 17.78 | 16.68 | 4 |
| BODU | Chad | PSA5 | soil sediment | 0.71785 | -12.6 | 18.87 | 16.87 | 4 |
| Bod 51 | Chad | PSA5 | soil sediment | | -12.2 | 19.07 | 17.43 | 6 |
| Bod 51_duplicate | Chad | PSA5 | soil sediment | 0.72129 | -12.0 | 19.07 | 17.43 | 6 |
| Sudan | Sudan | PSA6 | river sediment | 0.70567 | | 28.66 | 20.92 | 7 |

| Sudan | Sudan | PSA6 | river sediment | 0.70661 | | 28.66 | 20.92 | 7 |
|---|---|---|---|---|---|---|---|---|
| Main Nile, 3rd Cataract | Sudan | PSA6 | river sediment | 0.70497 | 1.7 | 30.41 | 19.94 | |
| Main Nile, 3rd Cataract | Sudan | PSA6 | river sediment | 0.70536 | | 30.41 | 19.94 | 8 |
| Main Nile, 3rd Cataract | Sudan | PSA6 | river sediment | 0.70614 | -0.8 | 30.41 | 19.94 | |
| Main Nile, 3rd Cataract | Sudan | PSA6 | river sediment | 0.70591 | | 30.41 | 19.94 | |
| Egypt1 | Egypt | PSA6 | soil sediment | | -9.2 | 30.52 | 22.67 | 2 |
| Main Nile, Ghaba | Sudan | PSA6 | river sediment | 0.70516 | | 30.75 | 18.14 | |
| Main Nile, Ghaba | Sudan | PSA6 | river sediment | 0.70508 | | 30.75 | 18.14 | |
| W. Milk, Ed Debba | Sudan | PSA6 | river sediment | 0.70743 | -7.5 | 30.89 | 17.91 | |
| W. Milk, Ed Debba | Sudan | PSA6 | river sediment | 0.70694 | | 30.89 | 17.91 | |
| W. Milk, Ed Debba | Sudan | PSA6 | river sediment | 0.71563 | -7.3 | 30.89 | 17.91 | |
| W. Milk, Ed Debba | Sudan | PSA6 | river sediment | 0.71691 | | 30.89 | 17.91 | |
| Main Nile, Gureir | Sudan | PSA6 | river sediment | 0.70526 | -2.9 | 31.69 | 18.31 | |
| Main Nile, Gureir | Sudan | PSA6 | river sediment | 0.70507 | | 31.69 | 18.31 | 8 |
| Main Nile, Karima | Sudan | PSA6 | river sediment | 0.70469 | 1.2 | 31.85 | 18.53 | |
| Main Nile, Karima | Sudan | PSA6 | river sediment | 0.70506 | | 31.85 | 18.53 | |
| Nile, 6Cataract | Sudan | PSA6 | river sediment | 0.70546 | 1.2 | 32.69 | 16.33 | |
| Nile, 6Cataract | Sudan | PSA6 | river sediment | 0.70566 | | 32.69 | 16.33 | |
| Blue Nile, Khartoum | Sudan | PSA6 | river sediment | 0.70513 | 0.7 | 32.70 | 15.47 | |
| Blue Nile, Khartoum | Sudan | PSA6 | river sediment | 0.70546 | | 32.70 | 15.47 | |
| Blue Nile, Khartoum | Sudan | PSA6 | river sediment | 0.70516 | 0.7 | 32.70 | 15.47 | |
| Assouan_bank | Egypt | PSA6 | river sediment | 0.70594 | -3.4 | 32.88 | 24.20 | 5 |
| Assouan_island | Egypt | PSA6 | river sediment | 0.70580 | 3.4 | 32.88 | 24.20 | 5 |
| Blue Nile, Wad Madani | Sudan | PSA6 | river sediment | | -0.3 | 33.50 | 14.44 | |
| Blue Nile, Wad Madani | Sudan | PSA6 | river sediment | 0.70551 | | 33.50 | 14.44 | |
| Atbara, Abu Ammar | Sudan | PSA6 | river sediment | 0.70433 | 2.3 | 34.21 | 17.53 | |
| Atbara, Abu Ammar | Sudan | PSA6 | river sediment | 0.70470 | | 34.21 | 17.53 | 8 |
| Derudeb, Derudeb | Ethiopia | PSA6 | river sediment | 0.70504 | | 36.12 | 17.98 | |
| Gash, Kassala | Sudan | PSA6 | river sediment | 0.70513 | -4.2 | 36.36 | 15.50 | |
| Gash, Kassala | Sudan | PSA6 | river sediment | 0.70496 | | 36.36 | 15.50 | |
| Gash, Kassala | Sudan | PSA6 | river sediment | 0.70577 | -2.4 | 36.36 | 15.50 | |

**Table 3: Soil and river samples located in the Potential Source Areas for dust generation (PSAs). Headers from left to right: Labels = name of the sampling location or sample; Region = country where the samples were taken; Location = name of the PSA (see figure 1); Sample type = soil or river sediment; Isotopic ratios of Sr and Nd; Longitude and Latitude (decimal degrees); Ref. = reference publications. These data were used to determine and plot the statistical values in figure 4. References: 1: Grousset et al. (1992), 2: Grousset and Biscaye (2005), 3: Grousset et al. (1998), 4: Gross et al. (2016), 5: Revel et al. (2010), 6: Abouchami et al. (2013), 7: Krom et al. (2002), 8: Padoan et al. (2011).**

|  | Time interval | Africa | Asia | Atlantic | Europe | Indian Ocean | Mediterranean | Total |
|---|---|---|---|---|---|---|---|---|
| **aerosol** | P | 26 |  | 17 | 7 |  | 18 | 68 |
| **bivalves** | P | 3 |  |  |  |  |  | 3 |
| **marine sediment** | LGM | 1 |  | 22 |  | 19 |  | 42 |
|  | P | 8 |  | 89 | 3 | 70 | 74 | 244 |
|  | S1 | 3 |  | 1 |  | 1 | 21 | 26 |
|  | S3 |  |  |  |  |  | 1 | 1 |
|  | S4 |  |  |  |  |  | 1 | 1 |
|  | S5 |  |  |  |  |  | 4 | 4 |
|  | S6 |  |  |  |  |  | 3 | 3 |
| **river sediment** | P | 98 | 6 |  | 42 |  |  | 146 |
|  | S1 |  |  |  |  |  | 1 | 1 |
| **soil sediment** | P | 60 |  | 10 |  |  |  | 70 |
| **trap sample** | P |  |  | 2 |  |  | 20 | 22 |
| **Total** |  | 199 | 6 | 141 | 52 | 90 | 143 | 631 |

**Table 4: Output table. Overview of the results obtained by applying sorting criteria, homogenizing the coordinates and determining the isotopic signature of specific time intervals.**
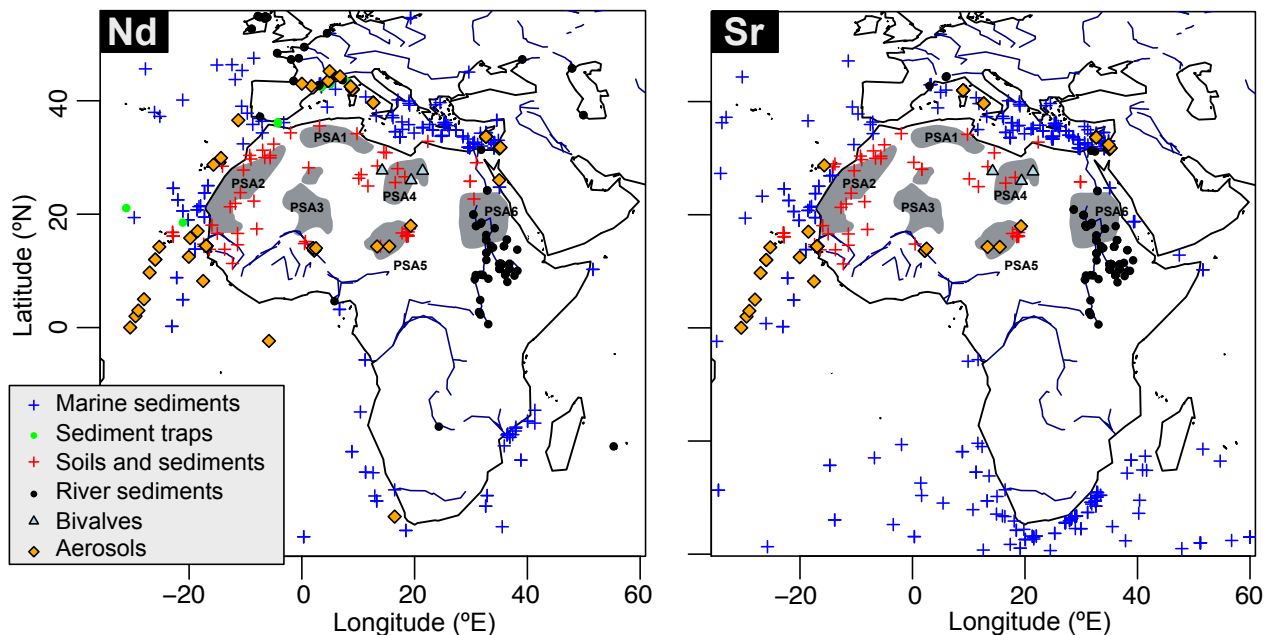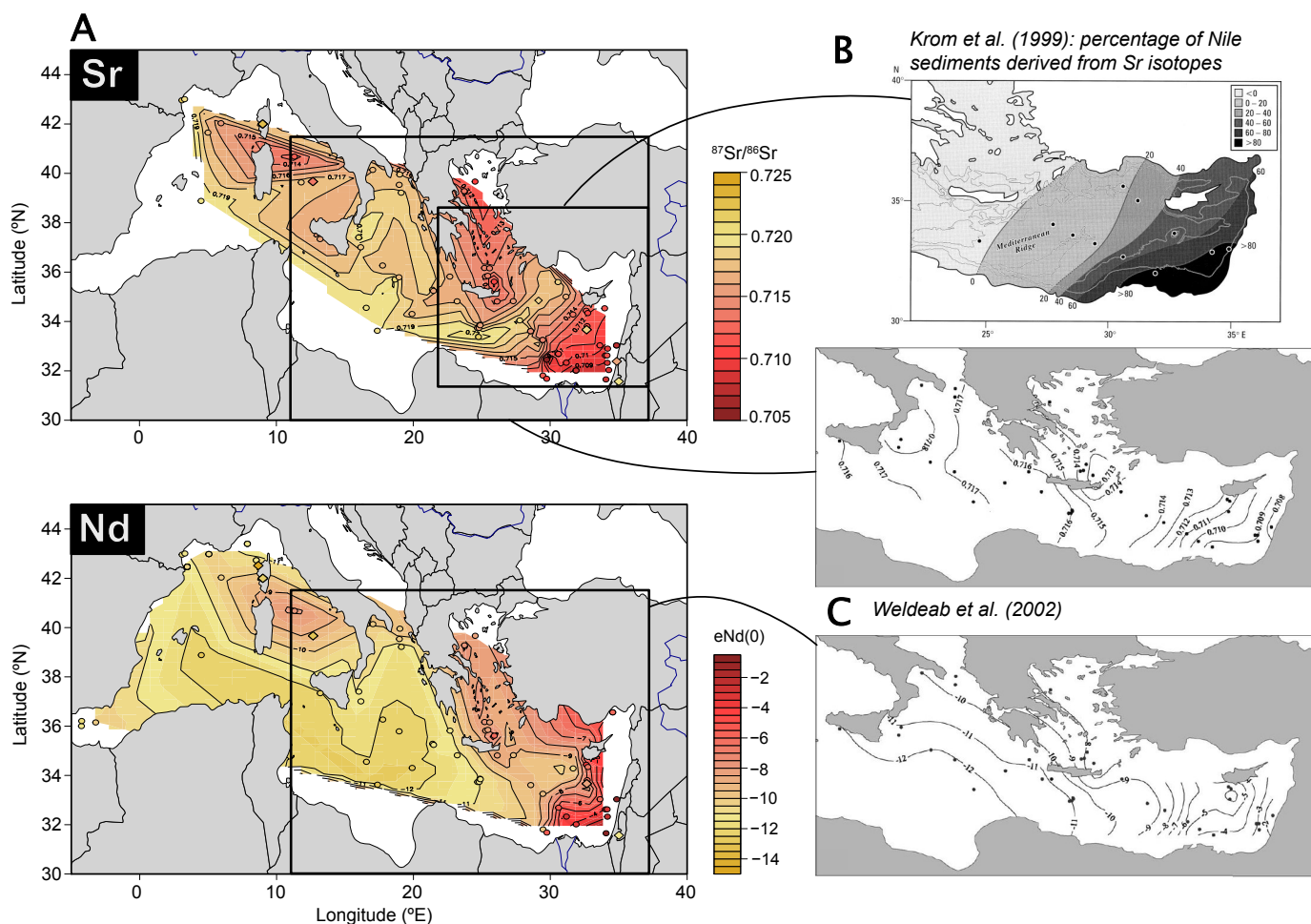
**Figures**



**Figure 1: Overview of the location of samples assembled in the database for Neodymium and Strontium isotope ratios. The sample types are indicated by different markers: blue crosses for marine sediments, green dots for sediment traps, red crosses for soil samples, black dots for river sediments (river banks or particulate matter), blue triangles for fossil bivalves (Osborne et al., 2008) and yellow diamonds for deposited dust samples. Main sources of dust (Potential Source Areas – PSAs) are indicated as grey underlines and were redrawn from Scheuvens et al. (2013). A complete list of reference is provided separately to the main dataset.**

**Figure 2:** Contour maps of the isotopic signature of marine surface sediments in the Mediterranean. A: contour maps produced using the assembled dataset for Strontium and Neodymium isotopes. The contour lines and filled contour maps were realised using individual surface (or core-top) sediment samples. Each sample is represented by a dot, which colour indicates its isotopic value according to the scale at the right of the panels. Aerosol samples are overlaid and represented by a diamond with a similar colour code. These maps are compared to previous contour maps from Krom et al. (1999b) (where the Sr isotopes to calculate a percentage of surface sediments derived from the Nile River runoff) (B) and Weldeab et al. (2002a) (C), which were inspirational to this work. Their respective extend is reported on the maps in A.
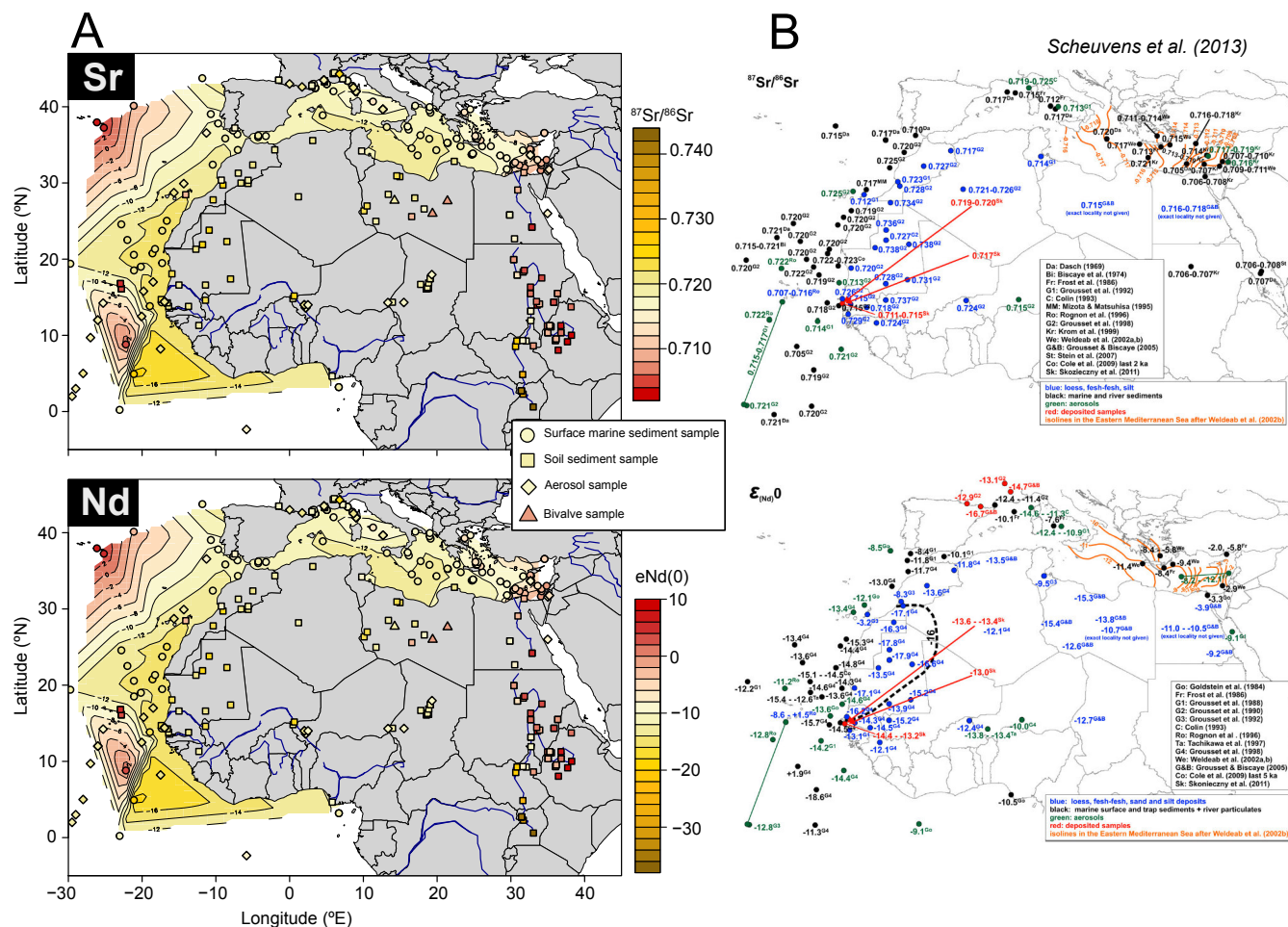
**Figure 3: Contour maps of the isotopic signature of marine and terrestrial sediment in the North African sector. A: comparison of the isotopic signature of marine surface sediments (contour maps) to that of terrestrial samples. Sample type is indicated by specific markers, which colour indicates its isotopic value according to the scale at the right of the panels: dots for marine surface sediments, squares for terrestrial (soil and river) sediment samples, diamonds for aerosols and triangles for fossil bivalves. B: maps from Scheuvens et al. (2013), which were inspirational to this work. The sample type is given by the colour of the markers: Blue for terrestrial samples, black for marine samples, green for aerosols (sediment traps) and red for deposited samples. Isotopic values are reported for each sample and the isolines from Weldeab et al. (2002b, cf. Figure 3) are also reported.**
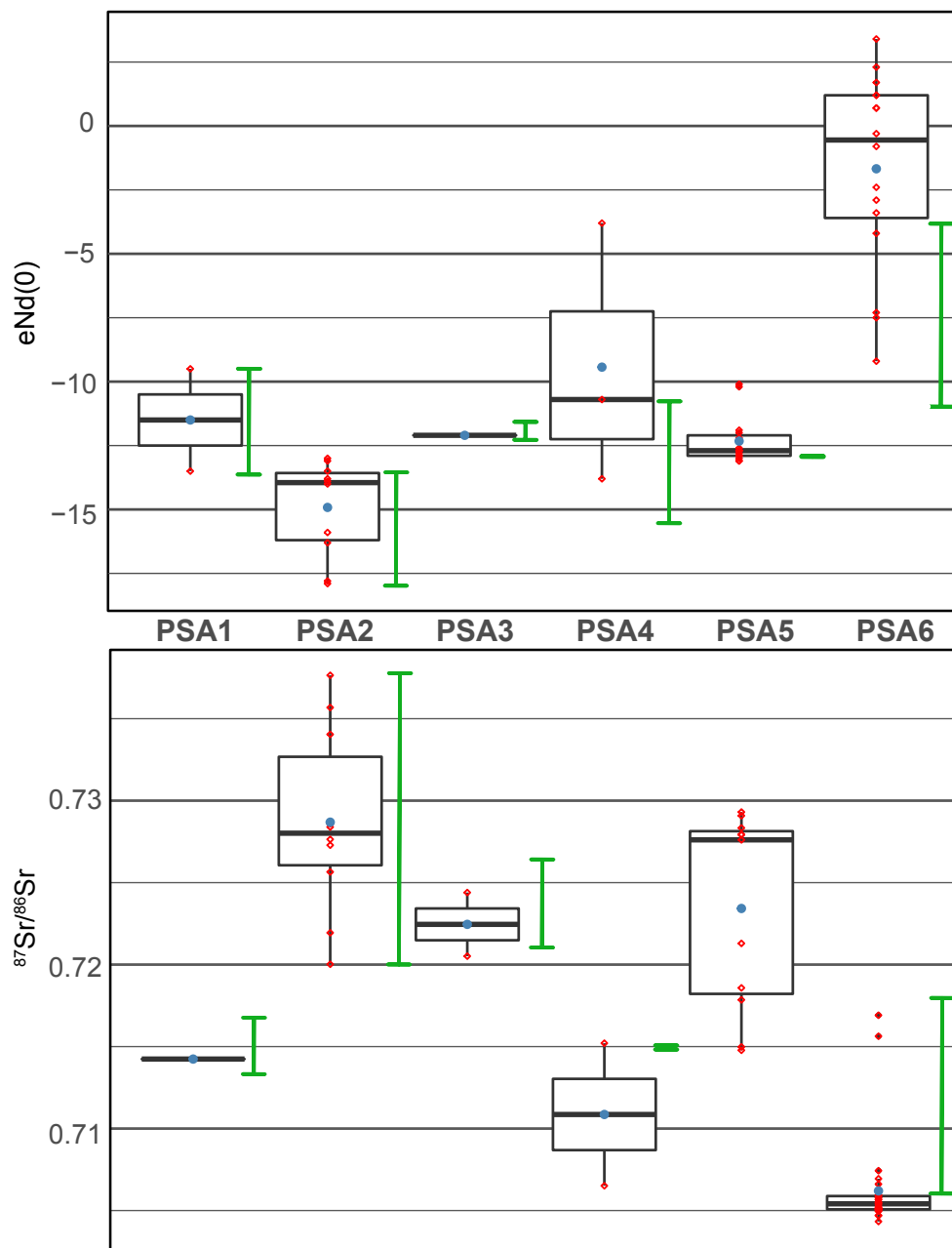
**Figure 4: Box and whiskers plot for the isotopic signatures of Potential Source Areas of dust generation (PSAs). After identifying samples that are located in each PSA (see table 3 and figure 1), the range and skewness of datasets in the PSA was analysed using box and whiskers plots and compared to the isotopic ranges reported by Scheuvens et al. (2013) (green bars). Data points are shown as red diamonds and the arithmetical mean is provided (blue dots). The rectangles indicate the upper and lower quartiles and the median.**